PROCEEDINGS OF SCIENCE

The Higgs boson and Electroweak Physics

Yves Sirois[*†]
Laboratoire Leprince-Ringuet, Ecole Polytechnique, CNRS-IN2P3
E-mail: yves.sirois@in2p3.fr

The discovery of the Higgs boson at a mass around 125 GeV by the ATLAS and CMS experiments at the LHC collider in 2012 establishes a new landscape in high energy physics. The analysis of the full data sample collected with pp collisions at 7 and 8 TeV during run I has allowed for considerable progress since the discovery. A review of the latest results is presented.

XXII. International Workshop on Deep-Inelastic Scattering and Related Subjects,
28 April - 2 May 2014
Warsaw, Poland

[*]Speaker.
[†]This paper mainly highlights recent results from the ATLAS and CMS experiments at the LHC.

PoS(DIS2014)020

1. Introduction: the standard model and the Higgs boson

The standard model (SM) of particle physics has provided a remarkably accurate description of numerous results from accelerator and non-accelerator based experiments over the past four decades. Yet, the question of how the W and Z gauge bosons acquire mass remained an opened question. This question could have jeopardized the validity of the theory at higher energies or, equivalently, at smaller distance scales. Understanding the origin of the electroweak symmetry breaking (EWSB), how the W and Z bosons acquire mass whilst the photon remains massless, has been set as one of the most important objectives of the Large Hadron collider (LHC) physics program at the birth of the project more than twenty years ago. The SM remained an unchallenged but incomplete theory for the interactions of particles [1] until the Large Hadron Collider (LHC) finally provided its first high energy proton-proton collisions at 7 TeV in 2010. The discovery of a Higgs boson at a mass of about 125 GeV by the ATLAS [2] and CMS [3] experiments in 2012 has now considerably changed the landscape.

The SM comprises matter fields, the quarks and leptons as the building blocks of matter, and describes their interactions through the exchange of force carriers: the photon for electromagnetic interactions, the W and Z gauge bosons for weak interactions, and the gluons for strong interactions. The electromagnetic and weak interactions are partially unified in the Glashow-Weinberg-Salam electroweak theory [4, 5, 6]. The gauge bosons are a direct consequence of the underlying gauge symmetries. It is sufficient to postulate the invariance under SU(2) $\times$ U(1) gauge symmetry in the electroweak sector to see emerging as a necessity the existence of the photon, for the electromagnetic interaction, and the W and Z bosons, for the weak interactions. The gauge symmetries are the essential pillars of the theory and thus must be preserved. This is only possible if the gauge bosons remain massless in the fundamental theory. Besides the question of the origin of the mass of vector bosons, the very existence of these massive bosons was threatening the theory at the TeV scale. In contrast to quantum electrodynamics where a renormalizable theory is obtained by injecting by hand the masses and charges measured at a any given scale, no such trick is possible for the weak interaction while preserving the gauge symmetries. The massive vector bosons lead to violation of unitarity for calculations at the TeV scale, unless something else is added. The SM with the gauge bosons and matter fields is incomplete. Additional structure is needed.

Since the advent of the electroweak theory, the Brout-Englert-Higgs mechanism [7, 8, 9, 10, 11] had been adopted as a solution to both the EWSB and the unitarization of the theory. In this mechanism, the introduction of a complex scalar doublet field with self interactions allows for a spontaneous EWSB. This leads to the generation of the W and Z masses (the weak boson acquire longitudinal degrees of freedom), and to the prediction of the existence of one physical Higgs boson (H). The fundamental fermions also acquire mass (the left- and right-handed chiralities become coupled) through Yukawa interactions with the scalar field when propagating in the physical vacuum. The mass m_{H} of the Higgs boson in the SM is not predicted by the theory, but general considerations [12] on the finite self-coupling of the Higgs field, the stability of the vacuum, and unitarization bounds suggest that it should be smaller than about 1 TeV. The shape of the scalar potential for the Higgs field that is responsible for EWSB depends on m_{H} and on the trilinear and quadrilinear self-couplings. In the SM, these are presumed to be fundamentally related. The trilinear coupling for the physical Higgs boson which enters for instance in di-H production is given

in the SM by $\lambda_{\mathrm{HHH}} = 3m_{\mathrm{H}}^2/v$, where $v = (\sqrt{2}G_F)^{-1/2} \approx 246$ GeV is the mean vacuum expectation value for the Higgs field. The existence of a scalar boson is sufficient to allow for an exact unitarization of the theory. But saving the theory has a cost: the arbitrariness m_{H} (and of the self-couplings) and the fact that the Higgs boson is not a gauge boson. Thus the mass m_{H} is not protected by any symmetry of the theory. The mass is sensitive to any new scale beyond the SM which could contribute in quantum fluctuations. The theory would have to be fine tuned to maintain m_{H} at the weak scale.

With these considerations, the scene is set to describe search and discovery of the Higgs boson at the LHC.

2. Higgs boson phenomenology

The total production cross sections for a SM Higgs [13] boson at the LHC are shown in Fig. 1 (left) for pp collisions. For $m_{\mathrm{H}} = 125$ GeV, the total production cross section is of about 22 pb at a centre of mass of $\sqrt{s} = 8$ TeV (about 17 pb at $\sqrt{s} = 7$ TeV). The Higgs boson is expected to be copiously produced. For this mass, about 87% of the Higgs bosons are produced via a gluon fusion (ggH) process involving a virtual top (or b) quark loop, 7.1% via vector boson fusion (VBF), 4.9% via "Higgstrahlung" (VH with V=W or Z), and 0.6 % in association with a top quark pair ($t\bar{t}$H).

The decay branching ratio for a SM Higgs boson [13] are shown in Fig. 1 (right). The WW di-boson decay dominates at high masses, for $m_{\mathrm{H}} > 135$ GeV. The WW and ZZ di-boson decays are the sole relevant modes for $m_{\mathrm{H}} > 2 \times m_{\mathrm{W}}$. At low mass, the $b\bar{b}$ and $\tau\bar{\tau}$ decays are the dominating modes. The intermediate mass range of $115 < m_{\mathrm{H}} < 135$ GeV offers the maximal sharing of the total decay width between the various decay channels. The decays in $c\bar{c}$ or gluon pairs are essentially inobservable as they are overwhelmingly swamped by di-jet QCD background. For $m_{\mathrm{H}} = 125$ GeV, this takes away from observation about 11.5% of the Higgs bosons. For this mass, the di-fermions represent about 64.0% of the decays; that is 58 % of the Higgs bosons decaying

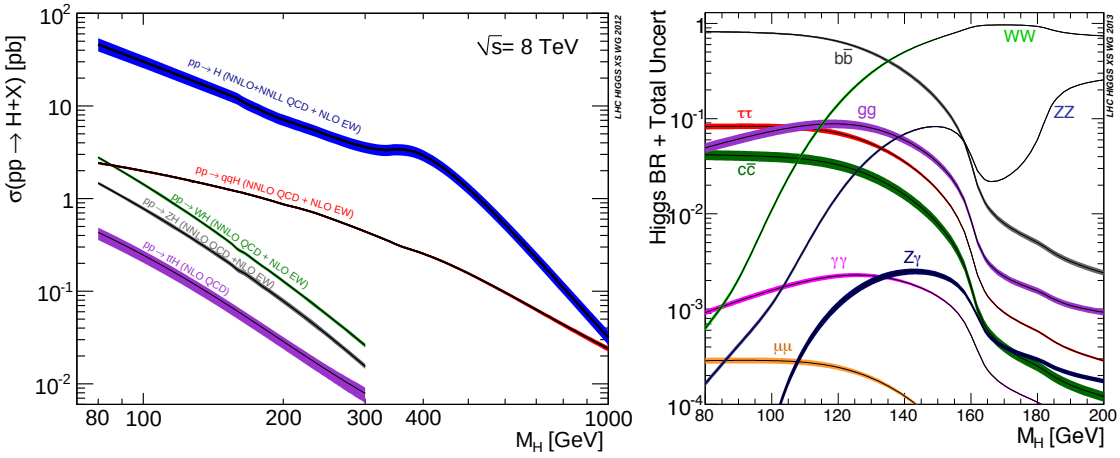

Figure 1: (*left*) Standard model Higgs boson production cross sections at $\sqrt{s} = 8$ TeV. (*right*) Branching ratio (BR) for the standard model Higgs boson. The plots are courtesy of Ref. [13] and reproduced here for convenience.

in $b\bar{b}$ pairs, and about 6 % in $\tau\bar{\tau}$ pairs. About 24.4% branching fraction is left for the di-bosons; that is 0.228% for $\gamma\gamma$, 21.5% for WW, and 2.64% for ZZ decays. Two high mass resolution decay modes offer the best discovery potential in the intermediate masse range, the $H \to \gamma\gamma$, and the decay chain $H \to ZZ^* \to 4\ell$ (in short $H \to 4\ell$) with at least one Z boson off-mass shell and $\ell = e, \mu$. While the $H \to \gamma\gamma$ decay is a rare decay mode, with it branching fraction of about 2×10^{-3} for $m_H = 125$ GeV, the $H \to 4\ell$ decay is even rarer, with a branching fraction of about 1.2×10^{-4} for $m_H = 125$ GeV when considering $4\ell = 4e, 4\mu$ and $2e2\mu$ final states.

For a given Higgs boson mass hypothesis, the sensitivity for the search and measurements in a given final state depends on the product of the production cross section and branching fraction to that final state, the signal selection efficiency, and the level of SM backgrounds in the relevant Higgs boson signal phase space.

The total production cross section at the LHC is about 20 times larger than the corresponding total cross-section at the Tevatron collider for $p\bar{p}$ collisions at $\sqrt{s} = 1.96$ TeV. With about 10 fb^{-1} of data collected in the D0 and CDF experiments by the end of the Tevatron lifetime, it was expected that the ATLAS and CMS experiments at the LHC would cover previous searches and take over with less than about 1 fb^{-1} of data. This occurred in 2011.

3. Higgs boson searches

The $H \to WW \to 2\ell 2\nu$, channel covers a wide mass range, but suffers from the lack of mass resolution due to the escaping neutrinos. This was the main channel used at the LHC for early searches of the Higgs boson. The main background processes are from non-resonant WW production and from top-quark production, including $t\bar{t}$ pairs and single-top-quark (mainly tW). By the time of the Lepton-Photon international conference in August 2011, both LHC experiments provided an exclusion at 95% CL of the Higgs boson for masses m_H around $2 \times M_W$, in a mass window extending beyond the reach of the Tevatron experiments. With up to 7.1 fb^{-1} and 8.2 fb^{-1} of data from the CDF and D0 experiments respectively, the Tevatron combination [21] excluded by then

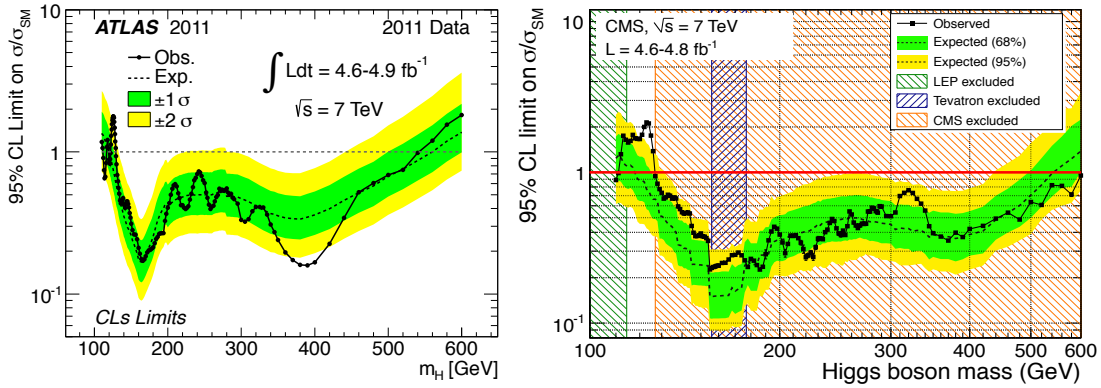

Figure 2: Upper limits from ATLAS and CMS using 2011 data with pp collisions at $\sqrt{s} = 7$ TeV. The 95% upper limits on the signal strength parameter $\mu = \sigma/\sigma_{SM}$ for the SM Higgs boson hypothesis is plotted as function of the Higgs boson mass .

the range $158-173$ GeV. From the $H \to WW$ channel alone, CMS using 1.5 fb^{-1} of pp collision data at $\sqrt{s} = 7$ TeV excluded [19] the existence of the SM Higgs boson in the range $147-194$ GeV, while ATLAS using 1.7 fb^{-1} of data excluded [20] the range $154-186$ GeV.

By fall 2011, both LHC experiments had deployed first analyses in all main decay channels covering the full mass range. At higher masses, the search in the $H \to WW$ channel is complemented by the use of the $H \to ZZ$ channel. The $H \to WW$ decay has two modes (W^+W^- and W^-W^+). Taking into account the differences in mass between the Z and W bosons, the partial width for $H \to ZZ$ is slightly less than that of one of the WW modes, i.e. less than half of $H \to WW$. The $H \to ZZ$ nevertheless provides the best sensitivity for $M_H \gg 2 \times M_Z$ from the combination of the $H \to ZZ \to 4\ell$ and $H \to ZZ \to 2\ell 2\nu$ channels, with $\ell = e, \mu$ and $\nu = \nu_e, \nu_\mu, \nu_\tau$. These channels were combined already at the end of the 2011 data taking campaign and this lead to the rather dramatic results shown in Fig. 2. The masses below 114.4 GeV were already excluded at 95% CL by the LEP experiments [22]. With less than 5 fb^{-1} of data collected at $\sqrt{s} = 7$ TeV in each experiment, the full mass range for masses $m_H > 130$ GeV was excluded. Somehow Nature has made it as difficult as possible, possibly hiding a cherished treasure in the most inaccessible range of $114.4 < m_H < 130$ GeV.

4. Higgs boson discovery

What followed now belongs to the history of science. Another 5 fb^{-1} of data was collected at $\sqrt{s} = 8$ TeV until June 2012 when the experimental data was re-analysed, leading to the discovery [2, 3] of a new boson around 125 GeV. The $H \to \gamma\gamma$ and the $H \to 4\ell$ play a special role in this low mass range as they provide a very good mass resolution for the reconstructed diphoton and four-lepton final states, respectively. More than twice as much data was collected by each of the experiments by the end of 2012 and this was enough to confirm that the new boson as properties compatible with those expected for the Higgs boson.

5. Understanding the standard model backgrounds

In parallel to the development of the Higgs boson analyses, there was considerable progress in understanding the SM backgrounds, both on the experimental side and for the accuracy of the theoretical calculations and Monte Carlo modelling. The path that leads from single W/Z boson and top quark pair production to electroweak diboson production and single top quark exchange had been first explored at the Tevatron collider. These SM studies have been pursued at an accelerated pace and considerably extended at the LHC.

The larger energy available at the LHC in the pp collision centre-of-mass opens up the phase space at high transverse momentum (p_T) for multiple jets recoiling against W/Z bosons. The W/Z + n jets production are major backgrounds to Higgs boson physics in multi-lepton final states when one or more jets are misidentified as leptons in the detector. These processes have now been measured with precision at the LHC up to $n \geq 4$jets and compared with SM expectation from full calculations now available at NLO. This is seen for example in Fig. 3 showing a compilation of recent CMS electroweak and top physics results, and comparison with theory expectation. Similar

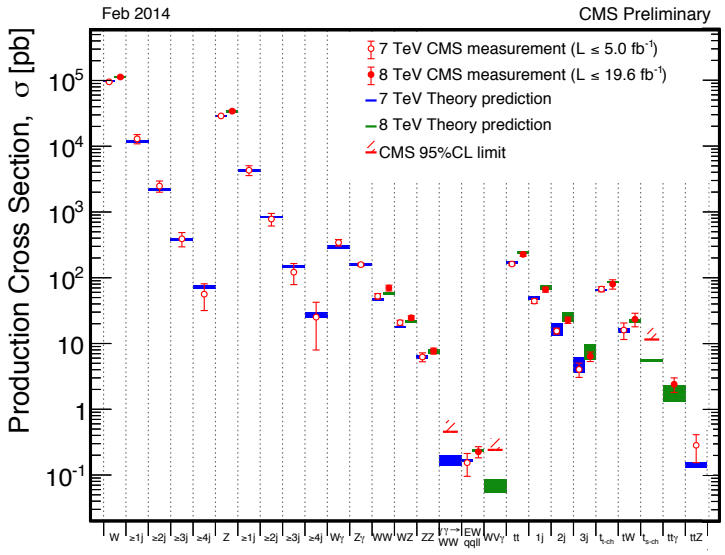

Figure 3: Production cross-section for electroweak bosons and top quarks measured by the CMS experiment in pp collisions at $\sqrt{s} = 7$ and 8 TeV.

results have been obtained by ATLAS. The di-boson production has been observed in each experiment in all possible modes: Wγ, Zγ, WW, WZ, and ZZ. The Table 1 gives the measured total cross sections for WW, WZ, and ZZ diboson production compared to theory expectation. All measurements are consistent with SM expectation. A slight excess (of about 20%) with a significance of about 2σ is observed by both experiments for the W^+W^- production cross sections at 8 TeV. The experimental studies have shown that the shapes of kinematic distributions (e.g. in invariant mass $m_{\ell\ell}$ of the lepton pair or $p_T^{\text{max.}}$ of the leading lepton, etc.) agree very well with expectation.

Final Higgs boson results from the run I are now becoming available and profit from the progress in understanding the SM background. The status is reviewed in the following.

Table 1: Measured total cross sections for WW, WZ, and ZZ diboson production in pp collisions at $\sqrt{s} =$ 8 TeV at the LHC. The WW cross section is measured via $ee, e\mu$ and $\mu\mu$ final states.

Process		$\sigma_{\text{tot}}^{meas.} \pm (\text{stat}) \pm (\text{syst}) \pm (\text{lumi})$ & $\sigma_{\text{tot}}^{theo.} \pm (\text{syst})$	Reference
$pp \to W^+W^- + X$	ATLAS	$71.4^{+1.2\,+5.0\,+2.2}_{-1.2\,-4.4\,-2.1}$	[14]
	CMS	$69.9 \pm 2.8 \pm 5.6 \pm 3.1$	[15]
	Theory	58.7 ± 3.0	MCFM NLO ($q\bar{q}$ & qg prod.), LO (gg prod.) + HWW at NNLO+NNLL
$pp \to WZ + X$	ATLAS	$20.3^{+0.8\,+1.2\,+0.7}_{-0.7\,-1.1\,-0.6}$	[16]
	CMS	$24.61 \pm 0.76 \pm 1.13 \pm 1.08$	[17]
	Theory	$21.91^{+1.17}_{-0.88}$	MCFM NLO; for $71 < M_Z < 111$ GeV
$pp \to ZZ$	ATLAS	$7.1^{+0.5}_{-0.4} \pm 0.3 \pm 0.2$	[18]
	CMS	$8.4 \pm 1.0 \pm 0.7 \pm 0.4$	[15]
	Theory	$7.7 \pm 0.4(\text{syst})$	MCFM NLO ($q\bar{q}$ prod.) & LO (gg prod.)

6. Higgs boson measurements using full LHC run I data

The ATLAS and CMS experiments have each published about 35 papers and about 100 "conference notes" or "physics analysis summary" notes related to the Higgs boson search and measurements, about half of these have become available over the past two years since the announcement of the discovery in July 2012. ATLAS first published in summer 2013 a combination of di-boson channels using all available run I data [23], but the results in individual decay channels have been since then superseded in some cases. A new combination of the five main decays channels and preliminary results in individual channels are now available [24]. CMS presented a preliminary combination using all available run I data in summer 2014 [25] which rely on a final set of run I results for each of the main five decays channels. These results are discussed below.

6.1 High resolution channels and the Higgs boson mass

The mass of the Higgs boson is determined by combining two discovery channels with excellent mass resolution, namely $H \to \gamma\gamma$ and $H \to ZZ^* \to 4\ell$. The mass resolution $\Delta M/M$ in each of these channels is expected to be in the range 1-2% from experimental effects. The intrinsic width has a negligible contribution to the measured mass resolution at the Higgs boson resonance for a SM boson mass around 125 GeV.

The $H \to \gamma\gamma$ signal is characterized by a narrow signal mass peak over a large but smoothly falling background. The photons in background events originate from prompt non-resonant diphoton production or from jets misidentified as an isolated photon. Details concerning the event selection can be found for ATLAS in Ref. [23] and for CMS in Ref. [27]. In both experiments, the analyses are split in mutually exclusive event classes to target the different production processes. The classification differ in the details between the experiments but it follow similar principles. Requiring the presence of two forward jets with high common invariant mass and a large rapidity gap favours events produced by the VBF mechanism. Event classes designed to preferentially select VH (V = W or Z) require mainly the presence of isolated electrons, muons, or missing transverse energy E_T^{miss}, or a dijet system with an invariant mass consistent with m_W or m_Z. The remaining "untagged" events correspond mainly to the Higgs boson production via gluon fusion and represents more than 90% of the expected signal in the SM. In both experiments, the "untagged" events are further split in categories according to the kinematics of the diphoton system, and the event-by-event estimate of the diphoton mass resolution which depends on photon reconstruction in different $|\eta|$ ranges of the detectors. In total, the ATLAS and CMS analyses rely on more than 10 categories for each of the s$\sqrt{s} = 7$ and 8 TeV samples. With an unfavourable signal to background ratio (S/B « 1 in most categories), a key to the $H \to \gamma\gamma$ analyses is the energy calibration of photon. This is obtained by using the $Z \to ee$ candle and extrapolating to the relevant p_T range of photons, taking into account the effects from the different behaviour of photon-induced and electron-induced electromagnetic showers (e.g. shift of the longitudinal profile) in the detector. Overall, the analyses have an acceptance×efficiency of about 50% and the event categorisation is expected to improve the sensitivity by about a factor two with respect to a fully inclusive analysis. A clear Higgs boson signal resonance is observed around 125 GeV with a local significance for ATLAS [23] of 7.4σ, for a SM Higgs boson expectation of 4.3σ, and a local significance for CMS [27] of 5.7σ, for a SM Higgs boson expectation of 5.2σ.

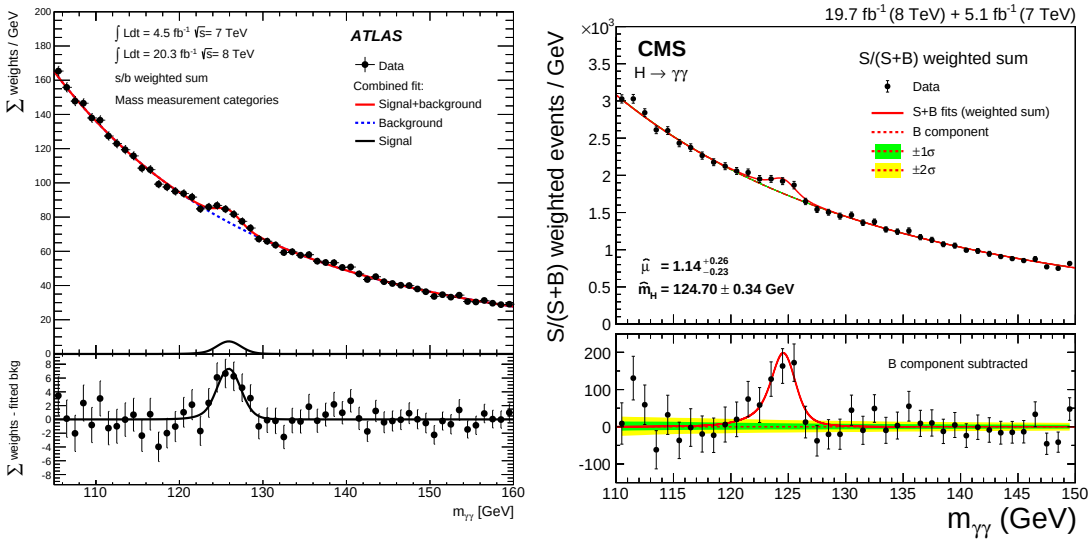

Figure 4: Distribution of the diphoton invariant mass measured in the H $\to \gamma\gamma$ analyses for run I data at 7 and 8 TeV. Combination of the event classes showing weighted data points with errors, and the result of the simultaneous fit to all categories from *(left)* ATLAS and *(right)* CMS experiments. In each case, the fitted signal plus background is shown along with the background-only component of this fit together, and the background subtracted weighted mass spectrum is shown in the bottom.

The diphoton invariant mass distribution measured by the experiments is shown in Fig. 4. For ATLAS, the plot shown here is from a recent paper Ref. [26] dedicated to the mass measurement and which uses an event categorization with only 10 categories (thus different from those used so far for the combination of channels for couplings and property measurements [23, 24]) optimized to minimize the expected uncertainty on the mass measurement, assuming a Higgs boson signal produced with the predicted SM yield. For CMS the same event categories and analysis from Ref. [27] making use of the definitive alignment and calibrations of the CMS detector for run I is used for the mass, coupling and property measurements.

The H $\to$ ZZ* $\to 4\ell$ signal is characterized by a narrow four-lepton ($4e, 2e2\mu$ or 4μ) mass peak over a small continuum background. Details concerning the event selection in this channel can be found for ATLAS in Ref. [23] and for CMS in Ref. [28]. The ATLAS and CMS analyses differ in the details but follow similar principles. The signal candidates are divided into mutually exclusive quadruplet categories, $4e$, $2e2mu$ and 4μ, to better exploit the different mass resolutions and different background rates arising from jets misidentified as leptons. Four well-identified and isolated leptons are required to originate from the primary interaction vertex to suppress the Z+ jet and $t\bar{t}$ instrumental backgrounds. With a very favourable expected signal to background ratio (S/B »1), a key to the H $\to 4\ell$ analyses is to preserve the overall efficiency while imposing lepton identification and isolation criteria sufficient to suppress the instrumental background well below the indistinguishable background from the non-resonant ZZ continuum. The fourth lepton (i.e. with lowest p_T) as its p_T peaking well below 10 GeV for $M_{\rm H} = 125$ GeV. A high lepton reconstruction efficiency is required down to the lowest p_T consistent with the rejection of instrumental background; in practice the lowest threshold is in the range 5 to 7 GeV. The electron reconstruction

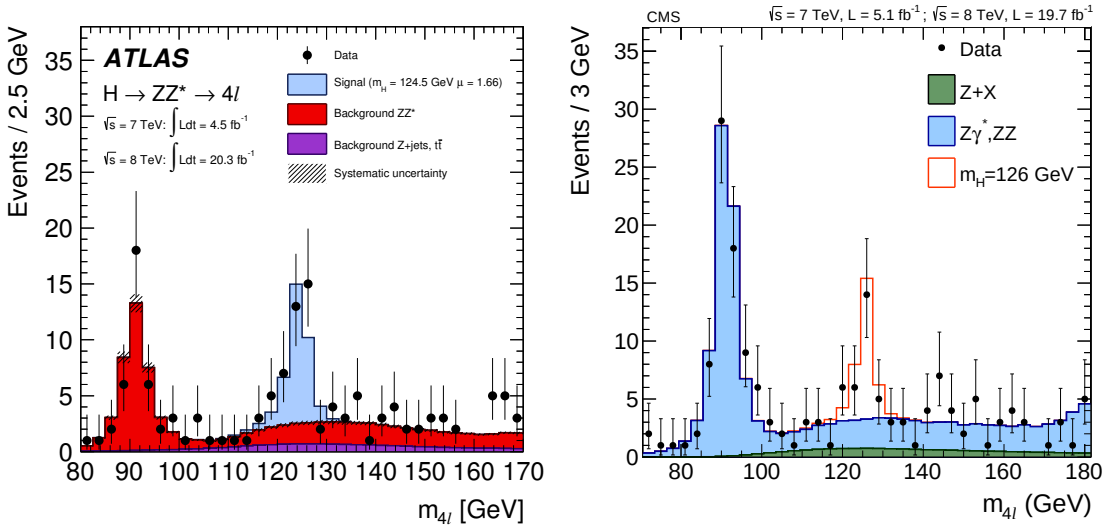

Figure 5: Distribution of the four-lepton invariant mass measured in the $H \to Z^{(*)}Z^* \to 4\ell$ analyses for run I data at 7 and 8 TeV, from *(left)* ATLAS and *(right)* CMS experiments. The plots show the sum of the $4e$, $2e2\mu$ and 4μ channels, with points with error bars representing the data, and shaded histograms representing the backgrounds. Superimposed in each case is an histogram for the Higgs boson signal expectation. This signal expectation is shown for a mass $m_H = 124.5$ GeV and a signal strength $\mu = \sigma_{obs.}/\sigma_{SM} = 1.66$ in the case of ATLAS, and for $m_H = 126$ GeV and the standard model expectation ($\mu = 1.00$) in the case of CMS.

makes use of rather sophisticated algorithms which combine the reconstructed track in the silicon tracker (using a gaussian sum filter technique dedicated to electrons) with clusters in the electromagnetic calorimeter, a categorization of electrons, etc. The energy scale is controlled using the $Z \to \ell\ell$ candle complemented by the validation at low p_T from J/ψ and Υ(nS). The signal candidates should contain two pairs of same flavour and opposite charge leptons ($\ell^+\ell^-$ and $\ell'^+\ell'^-$). For $M_H = 125$ GeV, the decay $H \to Z^{(*)}Z^*$ involves at least one Z boson off mass-shell (i.e. ZZ^*), and, for about 20% of the cross section, two Z boson off mass-shell (i.e. Z^*Z^*). The analysis thus accepts a leading Z boson (Z_1) reconstructed with masses down to 40 or 50 GeV, and a subleading one (Z_2) with masses down to 12 GeV. Overall, the analyses have an acceptance×efficiency of about 20 to 40% depending on the quadruplet category. Even more sophisticated statistical analysis techniques are used beyond the baseline selection of signal candidates. In CMS, kinematic discriminants are constructed using the masses of the two dilepton pairs and five angles, which uniquely define a four-lepton configuration in their centre-of-mass frame. These make use of leading order matrix elements for the signal and background hypothesis and are used to further separate signal and background. To enhance the sensitivity to the individual production mechanism, both experiments consider sub-categories to discriminate VBF and VH production from ggH production.

The 4ℓ invariant mass distribution measured by the experiments is shown in Fig. 5. For ATLAS, the plot shown is here again from a recent paper Ref. [26] dedicated to the mass measurement with lepton measurements and an analysis improved with respect to that used for the original combination of diboson channels [23], and different from that used for the new combination of channels [24]. For CMS the same event categories and analysis from Ref. [28] making use of the

Table 2: Signal strengths and mass measurements from the high resolution diboson channels at the LHC.

Expt.	Decay Channel	Signal Strength $\mu = \sigma_{meas.}/\sigma_{SM}$	Measured Mass (GeV) mass $\pm$ stat. $\pm$ syst.	Reference
ATLAS	H$\to\gamma\gamma$	$1.29^{+0.30}_{-0.30}$	$125.98 \pm 0.42(\text{stat}) \pm 0.28(\text{syst})$	[26]
	H$\to$ZZ*$\to 4\ell$	$1.66^{+0.45}_{-0.38}$	$124.51 \pm 0.52(\text{stat}) \pm 0.06(\text{syst})$	[26]
	Combined	—	$\mathbf{125.36 \pm 0.41}$	[26]
CMS	H$\to\gamma\gamma$	$1.14^{+0.26}_{-0.23}$	$124.7 \pm 0.31(\text{stat}) \pm 0.15(\text{syst})$	[27]
	H$\to$ZZ*$\to 4\ell$	$0.93^{+0.29}_{-0.25}$	$125.6 \pm 0.4(\text{stat}) \pm 0.2(\text{syst})$	[28]
	Combined	—	$\mathbf{125.03 \pm 0.30}$	[25]

definitive alignment and calibrations of the CMS detector for run I is used for the mass, coupling and property measurements. For the determination of the Higgs boson mass, both experiments make use of the uncertainty in the four-lepton mass estimated from detector information on a per-event basis. This is relevant because this uncertainty varies considerably over the small number of selected signal events. The measurements of the Higgs boson mass in the $\gamma\gamma$ and 4ℓ channels and for their combination is shown in Fig. 6. The measured mass values are listed in Table 2. The results are found to be remarkably consistent for each experiment and between the experiments. From the combination of $\gamma\gamma$ and 4ℓ channels, ATLAS obtains [26] $m_{\rm H} = 125.36 \pm 0.41$ while CMS obtains [25] $m_{\rm H} = 125.03 \pm 0.30$.

6.2 The Higgs boson width and intrinsic properties

Resonance width:

The intrinsic width ($\Gamma_{\rm H}$) of the Higgs boson in the SM is $\Gamma_{\rm H} \simeq 4.2$ MeV for $m_{\rm H} = 125$ GeV, corresponding to a lifetime $\tau^0_{\rm H} = \hbar/\Gamma_{\rm H} \simeq 2 \times 10^{-22} s$. This $\Gamma_{\rm H}$ is too small for a direct observa-

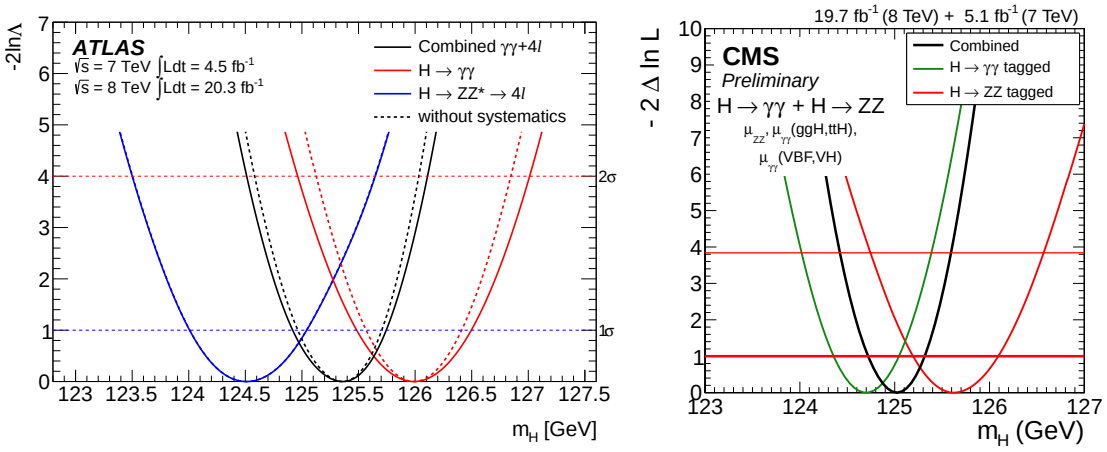

Figure 6: Scan of the likelihood test statistic versus the Higgs boson mass $m_{\rm H}$ for the H $\to \gamma\gamma$ and the H $\to 4\ell$ channels, and their combination, for *(left)* ATLAS, and *(right)* CMS.

tion at the peak where the resolution is completely dominated by detector resolution, while at the same time too large to allow for the observation of displaced vertices via its lifetime. At best, the experiment can verify that the lineshape at the resonance is consistent with a single narrow resonance. This has been explicitly done by the CMS experiment [27, 28] who sets direct limits of $\Gamma_H < 4.9$ GeV (from $H \to \gamma\gamma$) and $\Gamma_H < 3.7$ GeV (from $H \to 4\ell$). A sensitivity to a range of intrinsic width values of the order of Γ_H is nevertheless possible by profiting from the fact that the narrow width approximation fails for the production of a Higgs boson via gluon fusion (ggH). The off-shell production cross-section is sizeable and this has been exploited by the experiments in the ZZ channel.

In this channel, sizeable off-shell production of the Higgs boson arises from an enhancement in the decay amplitude in the vicinity of the Z-boson pair production threshold, and at higher masses from the top-quark pair production threshold. There is in addition at large mass a sizeable destructive interference with the production of a Z-boson pair from the continuum (i.e. with Z bosons coupling to quarks in a box diagram). Overall the ratio of the off-shell (above $2 \times m_Z$) to the on-shell cross section is of the order of 8%. This sizeable contribution of the Higgs boson off-shell is not as such surprising. The Higgs boson is essential for the unitarity of the theory and it must be there to play its role in canceling the bad high energy behaviour of the continuum diagrams. The on-shell and off-shell cross section can be approximated as:

$$\sigma^{\text{on-shell}}_{gg\to H\to ZZ^*} \approx \frac{g^2_{ggH} g^2_{HZZ}}{m_H \Gamma_H} \text{ and } \sigma^{\text{off-shell}}_{gg\to H^*\to ZZ^*} \approx \frac{g^2_{ggH} g^2_{HZZ}}{2m_Z} .$$

Thus, a measurement of the relative off-shell to on-shell signal production in the ZZ channel provides direct information on Γ_H. Using this idea [29], the CMS experiment has obtained [30] a constraint on the total width of $\Gamma_H < 22$ MeV (i.e. 5.4 times the expected value in the SM) at 95% CL. In a similar analysis ATLAS has obtained [31] a constraint at 28 MeV (6.7 times the expected value in the SM) at 95% CL.

Spin-parity:

Tests of the spin-parity state of the new boson at the LHC have been carried in the diboson channels by ATLAS [33] and CMS [32, 28, 27, 34]. Constraints on anomalous HVV interactions have in addition been established [35]. The observation of the new boson in the $H \to \gamma\gamma$ channel implies that the resonance must be a boson with spin 0 or 2. The spin 1 is excluded by the Landau-Yang theorem. Kinematic discriminants exploiting mass and angular correlations (as described above) have been also used by both ATLAS and CMS to test various spin-parity states for the signal hypothesis in the $H\to ZZ^*\to 4\ell$ and $H\to WW^*\to 2\ell 2\nu$ channels.

The CP-even 0^+ hypothesis is found to be favoured over any other pure spin-parity state hypothesis at a level of more than 3 standard deviations.

6.3 The Higgs boson signal rates and coupling measurements

Signal rates:

The signal strength modifiers $\mu = \sigma_{\text{meas.}}/\sigma_{\text{SM}}$ at the measured Higgs boson masses by the ATLAS [24] and CMS [25] experiments is shown in Fig. 7. Both the ATLAS and the CMS experiments have produced some results using the full run I data in the five main decay channels.

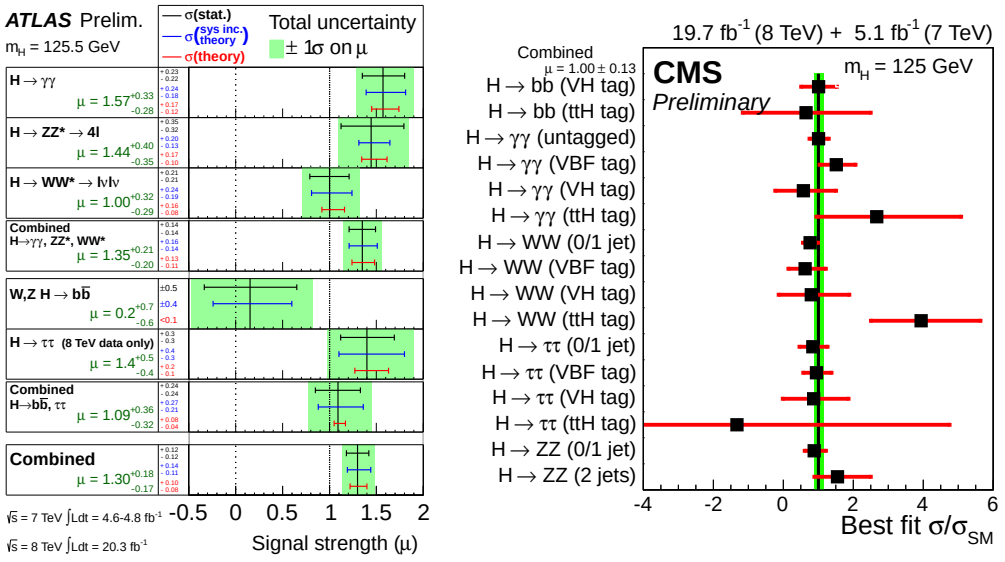

Figure 7: The signal strength modifiers $\mu = \sigma_{\text{meas.}}/\sigma_{\text{SM}}$ at the measured Higgs boson masses by the *(left)* ATLAS and *(right)* CMS experiments. For ATLAS the best-fit values are shown by the solid vertical lines with $\pm$ 1 standard deviation uncertainties indicated by green shaded bands, and the contributions from statistical uncertainty (top), the total (experimental and theoretical) systematic uncertainty (middle), and the theory uncertainty from QCD scale, PDF, and branching ratios (bottom) indicated within the bands. For CMS, the best fit value for the combination is shown as a solid vertical line and the overall uncertainty as a vertical band; the points are the results from sub-combinations by predominant decay mode or production mode tag. The uncertainties include both statistical and systematic uncertainties.

Besides the $\gamma\gamma$, ZZ, and WW di-boson channels which were the main contributors to the original discovery and have been exploited for the determination of the Higgs boson mass, intrinsic width, and spin-parity state, evidence has been found for the H$\to \tau\tau$ decay. In this H$\to \tau\tau$ channel, CMS observes [37] an excess with a significance of 3.2σ (3.7σ expected) and measures a signal strength of $\mu = 0.78 \pm 0.27$. ATLAS observes [38] an excess with a significance of 4.1σ (3.2σ expected) and measures a signal strength of $\mu = 1.4^{+0.5}_{-0.4}$. The top quark is involved in the main production channel. Indirect evidence for the Higgs boson coupling to the top quark is thus obtained from the observation of the ggH production. The other heavy fermions of the third generation, the b quark and the τ lepton, are involved in the dominating Higgs boson decay modes. A combination of the bb and $\tau\tau$ decay channels by CMS [41] yields an evidence for the coupling to these fermions at 3.8σ (4.4σ expected). The evidence for the H$\tau\tau$ coupling combined with the null evidence so far for the H$\mu\mu$ coupling [42, 43] implies that the new boson has non-universal family couplings. The new scalar field plays a role in the origin of fermion families.

The statistics in the VH production mode is too small at the LHC to establish at this stage a direct evidence for H$\to bb$. The analyses have nevertheless been carried by both experiments. An excess of signal candidates is observed by CMS [39] with a significance of 2.1σ (2.3σ expected) and by ATLAS [40] with a significance of 0.36σ (1.64σ expected). The most significant evidence so far for H$\to bb$ comes from the CDF and D0 experiments at the Tevatron. Combining their

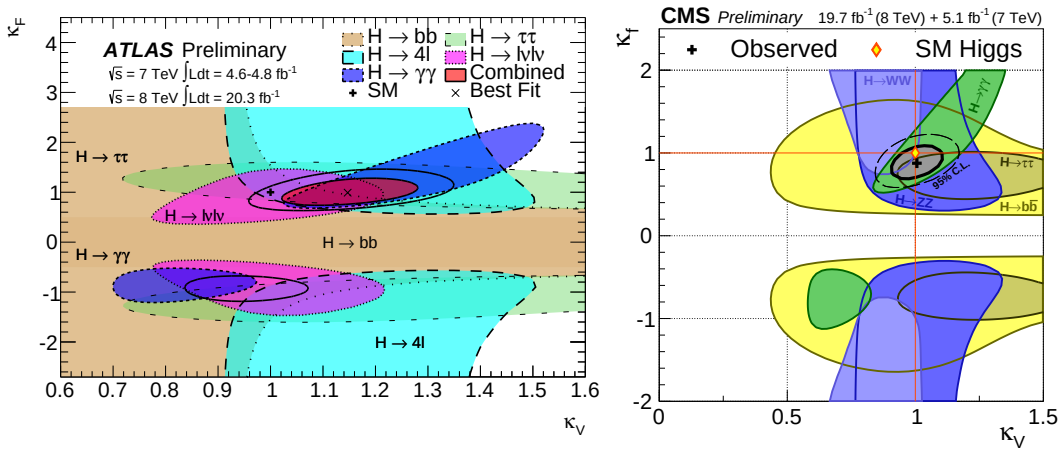

Figure 8: The 68% contours for individual decay channels (bounded colored regions) and for the overall combination (thick curves) in the correlation plane (κ_V, κ_F), the coupling scale factors for bosons (κ_V) and fermions (κ_F), from *(left)* ATLAS and *(right)* CMS. The standard model expectation is indicated at $(\kappa_V, \kappa_F) = (1,1)$. The likelihood scans are shown in the two quadrants, assuming either like signs $(+,+)$ or unlike signs $(+,-)$.

analyses in the VH production modes, the experiments [44] find an excess of signal candidates with a significance of 2.8σ at the LHC mass $m_{\mathrm{H}} = 125$ GeV, and a maximum local significance of 3.3σ at 135 GeV.

Couplings:

The production×decay for the Higgs boson at the LHC are always sensitive to a combination, linear at LO, of two couplings. Thus some model assumptions are required to disentangle the effects of each coupling. This is done following the prescription of the LHC Cross Section Working group. A narrow width approximation such that $\sigma \times \beta_i = \sigma_i \times \Gamma_i / \Gamma_{\mathrm{H}}$ is considered and SM "kappa" modifiers are introduced for the production, $\kappa_i^2 = \sigma_i / \sigma_i^{\mathrm{SM}}$, and decay $\kappa_j^2 = \Gamma_j / \Gamma_i^{\mathrm{SM}}$, with $\kappa_{\mathrm{H}} = (\sum \kappa_j^2 \Gamma_j^{\mathrm{SM}}) / \Gamma_{\mathrm{H}}^{\mathrm{SM}}$. Various benchmark scenarios are then studied [24, 25]. The ATLAS and CMS constraints on the Higgs boson coupling to fermions $(\kappa_f = \kappa_\ell = \kappa_q)$ and electroweak bosons $(\kappa_V = \kappa_{\mathrm{W}} = \kappa_{\mathrm{Z}})$ are shown in Fig. 8. The results are consistent with the expectation for the SM Higgs boson.

7. Conclusions and the aftermath

The boson discovered in 2012 at the LHC by the ATLAS and CMS experiments has properties so far consistent with the Higgs boson in a minimal scalar sector of the standard model, as expected from the Brout-Engler-Higgs mechanism for spontaneous electroweak symmetry breaking. The couplings to fermions (of the third generation) has been verified to ≈10-30% precision. The custodial symmetry which fixes the relative couplings of the Higgs boson to W and Z bosons is verified to 15%. The existence of a boson with non-universal family couplings is established via the evidence for H$\to \tau\tau$ and the null evidence for H$\to \mu\mu$. The existence of a scalar field, the

symmetry breaking mechanism, and the Higgs boson, provide an explanation for the origin of the Z and W and ordinary fermion masses and solves (or postpones to much higher energy) the problem of the unitarization of the theory. It marks the triumph of the weak couplings in the history of matter in the universe; a culmination of a reductionism strategy which has evolved from questions of the structure of matter to questions on the very origin of interactions (local gauge symmetries) and matter (interactions with Higgs field).

But there still remain the questions of the origin and stabilization of its mass at the weak scale. This question of a "natural" stabilization of the Higgs boson mass had been a central incentive for the developments of theories beyond the standard model (BSM) for many decades. In so-called "Technicolor" theories, one assumes that the SM is only an effective theory which breaks up at the TeV scale where a new strong interaction sets in. In so-called "extra dimension" theories, the validity of the SM is assumed to be limited at the TeV scale where strong effects of quantum gravity propagating in all dimensions would set in. Supersymmetric theories offer in principle a more satisfactory solution in the scalar sector. The self-coupling can possibly be expressed in a combination of gauge couplings in such theories such that the scalar sector is strongly constrained, e.g. with a predicted mass for the lightest, possibly SM-like, neutral Higgs boson. The stabilization of the Higgs scalar boson is obtained, despite the introduction of the new scale for the breaking of the supersymmetry, by exact cancellations of the contributions of the new supersymmetric particles, the partners of ordinary fermions and bosons.

The forthcoming data taking periods at higher pp centre-of-mass energies and higher integrated luminosity could allow for the observation of deviations from expectation or for the direct discovery of extra structure in the scalar sector, beyond the minimal sector of the standard model.

References

[1] Particle Data Group Collab., "Review of particle physics", J.Phys. G37 (2010) 075021, 1422pp.

[2] ATLAS Collab., "Observation of a new particle in the search for the standard model Higgs boson with the ATLAS detector at the LHC", Phys. Lett. B 716 (2012) 1.

[3] CMS Collab., "Observation of a new boson at a mass of 125 GeV with the CMS experiment at the LHC", Phys. Lett. B 716 (2012) 30; *idem*, "Observation of a new boson with mass near 125 GeV in pp collisions at $\sqrt{s} = 7$ and 8 TeV", JHEP 06 (2013) 081.

[4] S. L. Glashow, "Partial-symmetries of weak interactions", Nucl. Phys. 22 (1961) 579.

[5] S.Weinberg, "A Model of Leptons", Phys. Rev. Lett. 19 (1967) 1264.

[6] A. Salam, "Weak and electromagnetic interactions", in Elementary particle physics: relativistic groups and analyticity, N. Svartholm, ed., p. 367. Almqvist & Wiskell, 1968. Proceedings of the eighth Nobel symposium.

[7] F. Englert and R. Brout, "Broken symmetry and the mass of gauge vector mesons", Phys. Rev. Lett. 13 (1964) 321.

[8] P.W. Higgs, "Broken symmetries, massless particles and gauge fields", Phys. Lett. 12 (1964) 132. *idem*, "Broken symmetries and the masses of gauge bosons", Phys. Rev. Lett. 13 (1964) 508.

[9] [G. S. Guralnik, C. R. Hagen, and T.W. B. Kibble, "Global conservation laws and massless particles", Phys. Rev. Lett. 13 (1964) 585.

[10] P.W. Higgs, "Spontaneous symmetry breakdown without massless bosons", Phys. Rev. 145 (1966) 1156.

[11] T.W. B. Kibble, "Symmetry breaking in non-Abelian gauge theories", Phys. Rev. 155 (1967) 1554.

[12] J. M. Cornwall, D. N. Levin, and G. Tiktopoulos, "Uniqueness of spontaneously broken gauge theories", Phys. Rev. Lett. 30 (1973) 1268; *idem*, "Derivation of Gauge Invariance from High-Energy Unitarity Bounds on the s Matrix", Phys. Rev. D 10 (1974) 1145: *erratum* Phys. Rev. D11 (1975) 972; C. H. Llewellyn Smith, "High-Energy Behavior and Gauge Symmetry", Phys. Lett. B 46 (1973) 233; B.W. Lee, C. Quigg, and H. B. Thacker, "Weak Interactions at Very High-Energies: The Role of the Higgs Boson Mass", Phys. Rev. D 16 (1977) 1519.

[13] LHC Higgs Cross Section WG, "Handbook of LHC Higgs Cross Sections: 3. Higgs Properties", S Heinemeyer (ed.) July 4 (2013) 404 pp.; e-Print: arXiv:1307.1347 *unpublished*.

[14] ATLAS Collab., "Measurement of the W^+W^- production cross section in proton-proton collisions at $\sqrt{s} = 8$ TeV with the ATLAS detector", ATLAS-CONF-2014-033 (July 2014) 24p.

[15] CMS Collab., "Measurement of the W^+W^- and ZZ production cross sections in pp collisions at $\sqrt{s} = 8$ TeV", Phys. Lett. B 721 (2013) 190-211.

[16] ATLAS Collab., "A Measurement of WZ Production in Proton-Proton Collisions at $\sqrt{s} = 8$ TeV with the ATLAS Detector", ATLAS-CONF-2013-021 (March 2013) 24p.

[17] CMS Collab., "Measurement of the WZ production cross section in the $\ell^+\ell^-\ell'\nu$ decay channel at $\sqrt{s} = 7$ and 8 TeV at the LHC", CMS PAS SMP-12-006 (July 2013) 16pp.

[18] ATLAS Collab., "Measurement of the total ZZ production cross section in proton-proton collisions at $\sqrt{s} = 8$ TeV in 20 fb^{-1} with the ATLAS detector", ATLAS-CONF-2013-020 (March 2013) 19pp.

[19] CMS Collab., "Search for the Higgs boson decaying to W^+W^- in the fully leptonic final state", CMS Physics Analysis Summary PAS HIG-11-014 (August 2011) 14pp.

[20] ATLAS Collab., "Search for the Standard Model Higgs boson in the $H \to WW^{(*)} \to \ell\nu\ell\nu$ decay mode ...", ATLAS Conference note CONF-2011-134 (August 2011) 39pp.

[21] The TEVNPH Working Group for the CDF and D0 Collaborations, "Combined CDF and D0 Upper Limits on Standard Model Higgs Boson Production with up to 8.2 fb^{-1} of Data", FERMILAB-CONF-11-044-E (August 2011) 34pp.

[22] . ALEPH, DELPHI, L3, and OPAL Collaborations, "Search for the Standard Model Higgs boson at LEP", Phys. Lett. B565 (2003) 61-75.

[23] ATLAS Collab., "Measurements of Higgs boson production and couplings in diboson final states with the ATLAS detector at the LHC", Phys. Lett. B726 (2013) 88-119.

[24] ATLAS Collab., "Updated coupling measurements of the Higgs boson with the ATLAS detector using up to 25 fb^{-1} of proton-proton collision data", ATLAS-CONF-2014-009 (March 2014 - Revised in May 2014) 33pp.

[25] CMS Collab., "Precise determination of the mass of the Higgs boson and studies of the compatibility of its couplings with the standard model", CMS-PAS-HIG-14-009 (July 2014) 31pp.

[26] ATLAS Collab., "Measurement of the Higgs boson mass from the $H\to\gamma\gamma$ and $H\to ZZ^*\to 4\ell$ channels with the ATLAS detector using 25 fb^{-1} of pp collision data", ATLAS-HIGG-2013-12 (June 2014) 37pp.; submitted to Physical Review D.

[27] CMS Collab., "Observation of the diphoton decay of the Higgs boson and measurement of its properties", CMS HIG-13-001 (July 2014) 77pp.; submitted to European Physical Journal C.

[28] CMS Collab., "Measurement of the properties of a Higgs boson in the four-lepton final state", Phys. Rev. D89 (2014) 092007.

[29] F. Caola and K. Melnikov, "Constraining the Higgs boson width with ZZ production at the LHC", Phys. Rev. D 88 (2013) 054024; N. Kauer, G. Passarino, "Inadequacy of zero-width approximation for a light Higgs boson signal", JHEP 08 (2012) 116; N. Kauer, "Inadequacy of zero-width approximation for a light Higgs bo-son signal", Mod. Phys. Lett. A 28 (2013) 1330015; J.M. Campbell, R.K. Ellis, C. Williams, "Bounding the Higgs width at the LHC using full analytic results for $gg \to e^+e^-\mu^+\mu^-$", JHEP 1404 (2014) 060.

[30] CMS Collab., "Constraints on the Higgs boson width from off-shell production and decay to Z-bosons", Phys. Lett. B736 (2014) 64-85.

[31] ATLAS Collab., "Determination of the off-shell Higgs boson signal strength in the high-mass ZZ final state with the ATLAS detector", ATLAS-CONF-2014-042 (July 2014) 30pp.

[32] CMS Collab., "Study of the Mass and Spin-Parity of the Higgs Boson Candidate via Its Decays to Z Boson Pairs", Phys. Rev. Lett. 110 (2013) 081803.

[33] ATLAS Collab., "Evidence for the spin-0 nature of the Higgs boson using ATLAS data", Phys. Lett. B. 726 (2013) 120-144.

[34] CMS Collab., "Measurement of Higgs boson production and properties in the WW decay channel with leptonic final states", JHEP 1401 (2014) 096.

[35] CMS Collab., "Constraints on anomalous HVV interactions using H$\to 4\ell$ decays", CMS PAS HIG-14-014 (July 2014) 47pp.

[36] CMS Collab., "Constraints on Anomalous HWW Interactions using Higgs boson decays to W^+W^- in the fully leptonic final state", CMS PAS HIG-14-012 (July 2014) 20pp.

[37] CMS Collab., "Evidence for the 125 GeV Higgs boson decaying to a pair of τ leptons", JHEP 1405 (2014) 104.

[38] ATLAS Collab., "Evidence for Higgs Boson Decays to the $\tau^+\tau^-$ Final State with the ATLAS Detector", ATLAS-CONF-2014-108 (November 2013) 50pp.

[39] CMS Collab., "Search for the standard model Higgs boson produced in association with a W or a Z boson and decaying to bottom quarks", Phys. Rev. D89 (2014) 012003.

[40] ATLAS Collab., "Search for the $b\bar{b}$ decay of the Standard Model Higgs boson in associated (W/Z)H production with the ATLAS detector", ATLAS-CONF-2013-079 (July 2013) 36pp.

[41] CMS Collab., "Evidence for the direct decay of the 125 GeV Higgs boson to fermions", Nature Phys. 10 (2014).

[42] ATLAS Collab., "Search for the Standard Model Higgs boson decay to $\mu^+\mu^-$ with the ATLAS detector", ATLAS-HIGG-2013-017 (June 2014) 22pp.; submitted to Phys. Lett. B.

[43] CMS Collab.. "Search for the standard model Higgs boson in the $\mu^+\mu^-$ decay channel in pp collisions at $\sqrt{s} = 7$ and 8 TeV", CMS-PAS-HIG-13-007 (October 2013) 24pp.

[44] CDF and D0 Collaborations, "Evidence for a particle produced in association with weak bosons and decaying to a bottom-antibottom quark pair in Higgs boson searches at the Tevatron", Phys. Rev. Lett. 109 (2012) 071804; *idem*, "Higgs boson studies at the Tevatron", Phys.Rev. D88 (2013) 052014.